Chemical Science

ROYAL SOCIETY OF CHEMISTRY

EDGE ARTICLE

View Article Online
View Journal

Cite this: DOI: 10.1039/d5sc09201a

All publication charges for this article have been paid for by the Royal Society of Chemistry

Single stereocenter inversion of a cyclic tetrapeptide enables the detoxification of lead-exposed mice

Tagwa A. Mohammed,[a] Luca Sauser,[ab] Erica Pedron,[a] Yaël A. Hodel,[a] Tadeáš Kalvoda,[c] Francesco Prisco,[d] Lubomír Rulíšek,[c] Jason P. Holland *[a] and Michal S. Shoshan *[ab]

Lead (Pb) poisoning remains a global public health challenge, yet approved chelating agents are limited by poor selectivity, suboptimal efficacy, and safety concerns. We previously reported cyclic tetrapeptides as metal-binding therapeutics for Pb detoxification. The lead scaffold, containing two cysteines and two β-aspartic acid residues, showed high aqueous solubility but failed to rescue Pb-poisoned human cells. In this work, we conducted mechanistic studies revealing that diminished intrinsic Pb(II) affinity and poor selectivity against competing Ca(II) ions constrained its activity. Guided by these insights, we synthesized two analogs: one lacking a carboxylate and another with an inverted chiral center. Both analogs demonstrated markedly improved Pb detoxification in human cells, surpassing the efficacy of clinically used chelators. Strikingly, oral administration of the diastereomeric analog to Pb-exposed mice lowered blood Pb levels by 55–62% and increased urinary Pb excretion by up to 3-fold compared with vehicle or standard-of-care treatments. These findings illustrate how rational structure–activity relationship optimization can deliver selective, effective peptide-based chelators, establishing a promising therapeutic strategy against Pb poisoning.

Received 24th November 2025
Accepted 4th March 2026

DOI: 10.1039/d5sc09201a

rsc.li/chemical-science

Introduction

Lead (Pb) poses a serious threat to human health and the environment. The World Health Organization (WHO) classifies Pb as one of the top ten chemicals of major public health concern.[1] It is responsible for approximately one million deaths each year[2] and is highly toxic, even at very low concentrations. As a result, no blood lead level (BLL) is considered safe.[2–4] The WHO recommends medical and environmental intervention at a BLL of 5 μg dL^{-1} or higher.[2] In 2021, the US Centers for Disease Control and Prevention (CDC) lowered this threshold to 3.5 μg dL^{-1},[5] emphasizing the harmful effects of Pb at any detectable level.

According to these thresholds, it is estimated that one in three children worldwide, or more than 800 million children, are affected by Pb poisoning.[3] In the USA alone, between 1.5 and 2.1 million children are affected.[6] In addition, more than 50 percent of US adults are estimated to have elevated BLLs.[7] Pb affects nearly every organ system in the human body. It is particularly harmful to the kidneys, liver, and the central nervous system (CNS).[4,8,9] Children are especially vulnerable because their brains and CNS are still developing. As a result, Pb exposure during early life can cause long-term cognitive and behavioral impairments.[3,4,9]

Pb(II) ion is the most prevalent oxidation state of Pb. Its toxicity under physiological conditions arises from several key mechanisms.[4,8] For instance, Pb(II) binds to thiolate and carboxylate groups in peptides and proteins, thereby inhibiting their biological functions. Pb(II) ions mimic Zn(II) chemistry and compete with this essential metal ion in metalloenzymes such as δ-aminolevulinic acid dehydratase (δ-ALAD), carbonic anhydrases, acetylcholine esterases, and Zn-finger proteins, compromising their structure and function.[4,8,9] Due to its similar ionic radius to Ca(II), Pb(II) can cross the blood–brain barrier (BBB), where it disrupts calcium-binding proteins and interferes with neurotransmitter release;[4,10,11] Finally, Pb(II) ions bind to cellular reducing agents such as glutathione (GSH), thereby elevating oxidative stress.[8,11,12]

For nearly a century, small-molecule chelating agents (CAs) have been developed to bind toxic metal ions, including Pb(II), and facilitate their excretion through renal or hepatobiliary pathways.[13] This chelation mechanism remains the only approved treatment strategy for addressing metal toxicity, including Pb poisoning.[14–16] The standard of care (SOC) drugs

[a]Department of Chemistry, University of Zurich, Winterthurerstrasse 190, 8057 Zurich, Switzerland. E-mail: michal@metalead.ch; jason.holland@chem.uzh.ch
[b]metaLead Therapeutics AG, Hochbergerstrasse 60C, 4057 Basel, Switzerland
[c]Institute of Organic Chemistry and Biochemistry, Czech Academy of Sciences, Flemingovo náměstí 2, 16610 Praha 6, Czech Republic
[d]Laboratory for Animal Model Pathology, Institute of Veterinary Pathology, Vetsuisse Faculty, University of Zurich, Winterthurerstrasse 268, 8057 Zurich, Switzerland

used for Pb detoxification are dimercaptosuccinic acid (DMSA) and ethylenediaminetetraacetic acid (EDTA). While these agents can reduce BLL in cases of severe poisoning, they have several major limitations. First, due to their low selectivity for Pb(II), they also bind other essential metal ions, such as Zn(II) and Ca(II), which can lead to side effects and reduced efficacy. Second, their poor cellular permeability limits their activity to the extracellular space, slowing chelation and reducing efficiency. Third, EDTA treatment is suspected to induce redistribution of Pb(II) ions to the brain.[14–16] Lastly, these two CAs function only at very high BLL values and are incapable of reducing lower, yet still dangerous BLLs. As a result of these shortcomings, DMSA and EDTA are prescribed only when the BLL exceeds 45 and 70 μg dL^{-1}, respectively, which is nine and 14 times higher than the intervention threshold recommended by the WHO.[2,17]

In response to these limitations, alternative Pb detoxification strategies have been explored, including small-molecule ionophores, biomimetic ligands, polymeric scavengers, and peptide-based binders.[12,18] While some of these approaches improve metal-binding affinity or oral bioavailability, many still suffer from limited selectivity against essential metal ions, insufficient intracellular activity, or poor *in vivo* efficacy.[19] Moreover, few candidates have demonstrated the ability to safely reduce Pb burden at low but clinically relevant BLLs, underscoring the continued need for selective, mechanistically informed chelation strategies.[20,21]

Short peptides have demonstrated significant potential as Pb binders for detection and remediation; however, they have not yet been studied for therapeutic applications.[22–30] In previous work, we developed several families of peptides for Pb detoxification.[31–33] Screening identified a promising cyclic tetrapeptide scaffold comprising two α-amino acids and two alternating β-amino acids, containing at least two Pb(II)-chelating functional groups (Fig. 1A).[31] Peptide **1**, composed of two cysteine and two β-alanine residues, showed the strongest activity, enhancing survival of Pb-poisoned *E. coli* by more than eightfold (Fig. 1B).[31,34] However, its low aqueous solubility

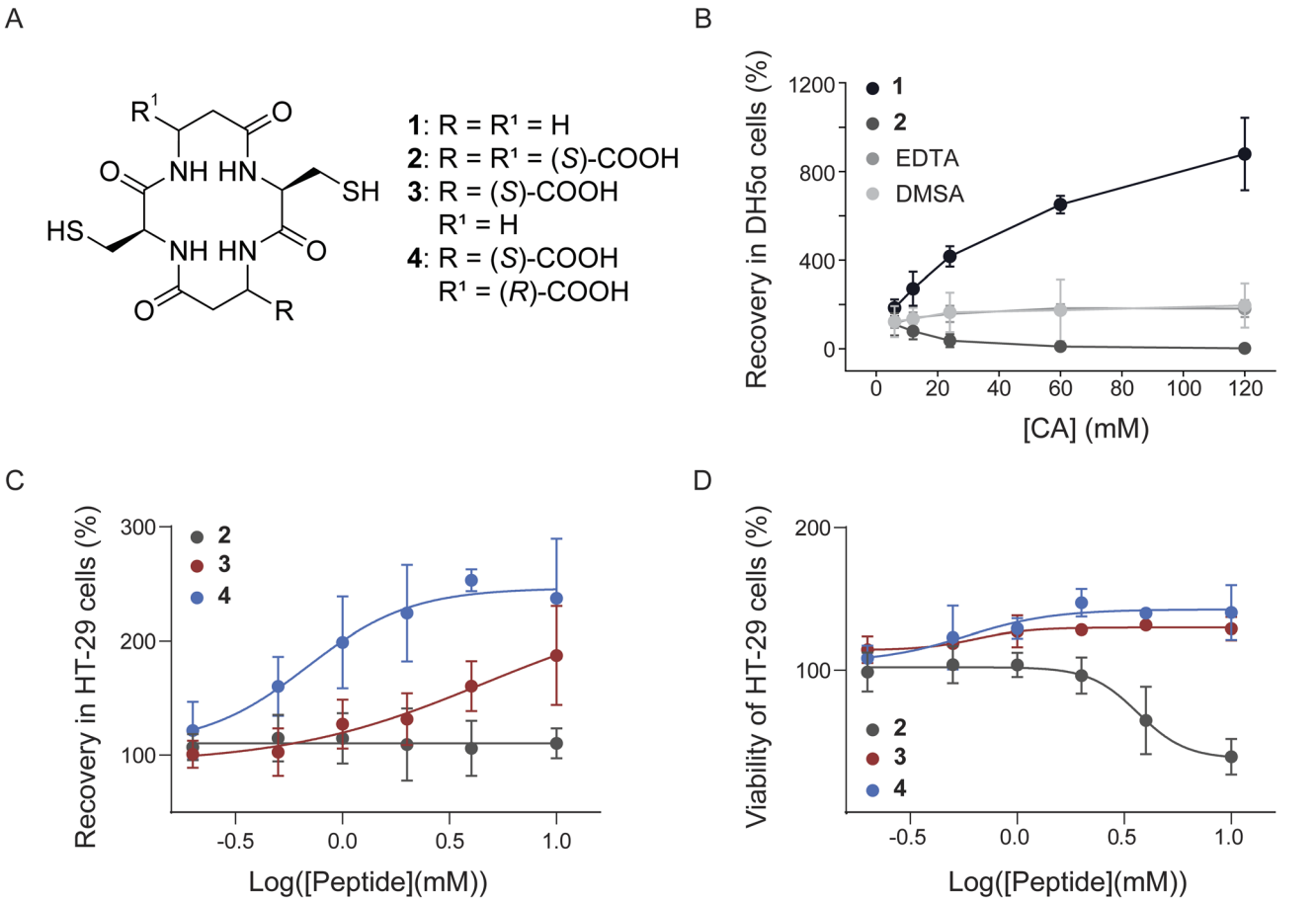

Fig. 1 (A) Chemical structures of peptides **1**–**4**. Peptides **1** and **2** have been reported previously[31] while peptides **3** and **4** are new. (B) Dose-dependent recovery of DH5α cells treated with $Pb(NO_3)_2$ (12 mM), followed by the administration of cyclic peptides **1** or **2** (as di-Na salts) or the SOC CA, DMSA (as di-Na salt). The CAs were added 5 h after the addition of Pb(II) ions; values are calculated relative to cells poisoned with Pb(II) ions as the negative control. Graph adopted from ref. 31. (C) Dose-dependent viability of HT-29 cells treated with **2**, **3**, or **4** (as di-Na salts). Values are mean ± SD of at least 3 independent repeats. The results for peptide 2 have been reported in ref. 31. (D) Dose-dependent recovery of HT-29 cells treated with $Pb(NO_3)_2$ (2 mM) followed by the administration of cyclic peptides **2**, **3**, or **4** (as di-Na salts; 1 h after the addition of Pb(II) ions; values are calculated relative to cells poisoned with Pb(II) ions as the negative control). The results for peptide **2** have been reported in ref. 31.

limited its potential as a CA.[34] Replacement of the β-alanine residues with β-aspartic acid yielded peptide **2** (Fig. 1A), which exhibited improved solubility but was ineffective and cytotoxic (Fig. 1B–D).[31,35]

In this work, we designed two analogs of **2** that differ in either the number of free carboxylic acid groups or their absolute configurations to better elucidate the reasons for the poor activity and high toxicity of peptide **2** and to further improve it through rational design. Comprehensive experimental studies on the three peptidic analogues, including cellular efficacy and cytotoxicity testing, mechanistic evaluations, and most importantly, efficacy studies of the best-performing peptide in mice, provided critical insights into the factors governing Pb(II) binding and detoxification. These findings underscore the importance of tuning both metal-ion affinity and selectivity to enable peptides to effectively reverse Pb poisoning, both *in vitro* and *in vivo*.

Materials and methods

Materials and reagents were of the highest grade available and purchased from ABCR, Sigma-Aldrich, TCI, or Fluorochem, and used without further purification. Amino acid building blocks were purchased from Merck, Bachem, Novabiochem, Senn, or ABCR and used as received. Water used for peptide preparation and purification was nanopure ("Milli-Q") prepared by a Barnstead GenPure system (ThermoFisher Scientific).

Solid-phase peptide synthesis

Solid-phase peptide synthesis (SPPS) was performed on 200–400 mesh CTC Polystyrene resin from ABCR.[36]

NMR spectroscopy

^{1}H and ^{13}C NMR spectra were recorded on a Bruker AV-NEO-400 or AVII-400 (400 MHz). Chemical shifts are reported in ppm using the solvent residual peak as reference (D_2O 4.79 ppm for ^{1}H, $CDCl_3$ 7.26 ppm for ^{1}H, and 77.16 ppm for ^{13}C). Assignment of the signals in the one-dimensional ^{1}H NMR spectra was confirmed when needed by two-dimensional NMR spectroscopy (COSY, TOCSY, NOESY, HSQC, HMBC).

Mass spectrometry

HR-MS-ESI measurements were performed on a timsTOF Pro TIMS-QTOF-MS instrument (Bruker Daltonics GmbH).

ICP-MS measurements were performed with an Agilent QQQ 8800 Triple quad ICP-MS spectrometer, equipped with a standard X-lens setting, nickel cones, and a "micro-mist" quartz nebulizer. The feed was 0.1 mL min^{-1}, and the RF power was 1550 W. Tune settings were based on the Agilent General Purpose method and only slightly modified by an autotune procedure using an Agilent 1 ppb tuning solution containing Li, Y, Ce, and Tl. Values are reported as the average of 30 sweeps, each repeated three times. Elements were measured in a "helium mode". All solutions were prepared from 60% HNO_3 (Merck 1.01518.1000 ultrapure), 30% HCl (Merck 1.01514.1000 ultrapure), or aqua regia (1 : 3 mixture of 60% HNO_3 and 30% HCl 1 : 3, ultrapure) and 18.2 MΩ Millipore water. Elements were measured against a serial dilution with the following standards: Pb: Merck 1.70313.0100 in 2% HNO_3, Ca: Merck 1.70344.0100 in H_2O. Merck 1.70324.0100, 2% HNO_3, was used as an internal standard.

Cell culture

Cell culture was conducted with human colon adenocarcinoma cells (HT-29) that were purchased from the ATCC. The cells were grown in a humidified 5% CO_2 atmosphere at 37 °C using RPMI-1640 with 25 mM HEPES, supplemented with 1% L-glutamine, 1% penicillin/streptomycin, and 10% FCS superior (standardized). Culture medium RPMI-1640-HEPES (with L-glutamine), penicillin (10.000 U mL^{-1}), and streptomycin (10 mg mL^{-1}) were purchased from Sigma Aldrich, Invitrogen, or BioConcept. Trypsin-EDTA (0.02%) in Ca(II) and Mg(II) deficient PBS (1 : 250) was purchased from Amimed. FCS superior was purchased from Oxoid AG and Biochrom AG. Crystal violet (CV) stain was purchased from Sigma Aldrich. CV assays were monitored on a Hidex Sense microplate reader.

UV-vis spectroscopy

UV-vis spectrophotometer titration, stability, and selectivity measurements were performed using a Lambda 850 UV-vis spectrophotometer (PerkinElmer) with an ultra-micro Suprasil quartz cuvette (Hellma) having a chamber volume of 100 μL and a path length of 10 mm. Wavelength scans were performed at 25 °C from 200 to 400 nm with a scan speed of 40 nm min^{-1}.

Isothermal titration calorimetry (ITC)

ITC experiments were performed on a VP-ITC MicroCalorimeter (Malvern) at 25 °C. The data were analyzed using the tailored Origin software (provided by the instrument's manufacturer) and fitted with one or two sets of binding-site models. Each measurement was independently repeated at least twice. The errors to the N and K_d values have been calculated by the manufacturer's software and are reported as-is.

Animal experiments

Mice experiments were conducted in accordance with an animal experimentation license approved by the Zurich Canton Veterinary Office, Switzerland (Jason P. Holland). Experimental procedures also complied with the ARRIVE 2.0 guidelines.[37] Female mice (C57BL/6, 20–25 g, 6–8 weeks old) were obtained from Charles River Laboratories Inc. (Freiburg im Breisgau, Germany) and allowed to acclimatize at the University of Zurich Laboratory Animal Services Center (LASC) vivarium for at least 1 week prior to experimentation. Mice were provided with food and water ad libitum. Mice were also randomized before the study.

Phenotyping

Phenotyping was performed on mice from two experimental cohorts. First, liver, brain, kidney, and femur were collected from mice administered $Pb(Ac)_2$ in drinking water and

subsequently treated with PBS (control group, $n = 5$), DMSA ($n = 5$), or peptide **4** ($n = 5$). Second, to evaluate potential phenotypic alterations associated with peptide **4** treatment alone, 5 mice treated exclusively with peptide **4** and four control mice treated with PBS alone were euthanized and subjected to a complete post-mortem macroscopic and histopathological examination. The following organs or tissues were systematically collected and examined: brain, heart, trachea and lungs, tongue, salivary glands, esophagus, stomach, duodenum, jejunum, ileum, caecum, colon, liver with gallbladder, pancreas, kidneys, urinary bladder, spleen, mandibular and mesenteric lymph nodes, thymus, bone marrow (femur, sternum), ovaries, uterus, vagina, skeletal muscle (M. quadriceps femoris, diaphragm), femoral bone, head with nasal cavity and teeth, spinal cord, thyroid gland, adrenal glands, skin and mammary gland). Tissue samples were fixed in 10% neutral buffered formalin immediately following euthanasia, routinely processed, and embedded in paraffin wax. Sections (3 μm thickness) were cut and stained with hematoxylin and eosin (HE) for histopathological evaluation.

Results and discussion

Cellular evaluation

To better understand why peptide **2** was inactive in reversing cellular Pb toxicity (Fig. 1C),[31] we synthesized two additional analogues: peptide **3**, which contains only one free carboxylic acid group (sequence: cyc-[Cys-βAsp-Cys-βAla]) was designed to maintain some polarity whilst limiting undesired metal binding, and peptide **4**, a diastereomer of **2** in which one βAsp residue is replaced by βDAsp (sequence: cyc-[Cys-βAsp-Cys-βDAsp]) was designed to control the spatial orientation of the carboxylate group, which will reduce steric strain and limit undesired metal binding events.[38] Both peptides were synthesized and purified by using procedures similar to those previously reported.[31,36]

Interestingly, when the peptides were incubated with human cells to examine their effect on cell viability, only peptide **2** exhibited cytotoxicity, particularly at high concentrations (Fig. 1C).[31] Peptides **3** and **4**, on the other hand, had no disruptive effect.[35] This toxicity may stem from the ability of peptide **2** to bind essential metal ions, such as Ca(II), thereby disrupting normal cellular function.

We then evaluated each peptide for its ability to recover Pb-poisoned human cells as an initial efficacy assessment.[36] Human colon cancer cells, being sensitive to Pb(II) exposure, were first incubated with 2 mM $Pb(NO_3)_2$. One hour later, peptides were added at concentrations ranging from 0.2 to 10 mM (0.1 to 5 equivalents). After 23 hours of additional incubation, cell viability was assessed and compared to that of Pb-exposed cells treated with vehicle (negative control; Fig. 1D) or to unexposed cells (positive control; Fig. S1).[36] While peptide **2** showed no recovery activity, peptide **3** exhibited partial restoration of viability, and peptide **4** was highly effective, increasing viability up to 240% relative to the negative control and reaching a complete rescue compared with the positive control (Fig. 1D and S1, respectively). These results highlight the critical role of the second carboxylate group and its configuration in achieving therapeutic efficacy. We hypothesize that significant differences in Pb-binding affinity and selectivity, combined with peptide stability (Fig. S6), were translated into these fundamental differences in the biological activity. To better understand the effect of such minor chemical alterations, we have studied the interactions between the various peptides and relevant metal ions.

Complex characterization

Affinity to Pb(II) ions. We first determined the binding affinities of peptides **2** and **4** toward Pb(II) ions using isothermal titration calorimetry (ITC).[39] This method has been selected as one of the most accurate for determining thermodynamic reaction parameters. Peptide **4** exhibited strong binding with a dissociation constant (K_d) of 2.2 nM, sixfold tighter than that of peptide **2**, highlighting the superior Pb(II)-binding affinity of **4** (Fig. 2A). ITC analysis also revealed that peptide **4** can bind two Pb(II) ions, possibly through independent coordination at two distinct sites, each involving a thiolate and a carboxylate group. This dual binding can be facilitated by a conformational arrangement that prevents interference between the two binding sites. In contrast, the ITC-derived binding stoichiometry for peptide **2** of 1.44 ± 0.03 was inconclusive, suggesting that a mixture of both 1 : 1 and 2 : 1 (Pb : peptide) complexes is possible (Fig. 2A).

To further investigate the interaction between these peptides and Pb(II) ions, we conducted UV titrations monitoring the ligand-to-metal charge transfer (LMCT) transitions of the S(3p) → Pb(6p) type upon incremental addition of $Pb(NO_3)_2$ (Fig. 2B).[36,40–42] Both peptides **2** and **4** showed features consistent with binuclear complex formation, as saturation was reached upon the addition of two equivalents of Pb(II) ions. This finding aligns with the ITC data of peptide **4**. However, in the case of peptide **2**, there is a minor misalignment between the two readouts. This apparent discrepancy likely reflects the coexistence of multiple binding species in solution. ITC reports an effective, population-averaged stoichiometry that integrates all thermodynamically relevant binding events, including partially occupied complexes, whereas UV-vis spectroscopy preferentially detects the fully metal-saturated complex responsible for the dominant spectral changes. Such differences between the two experiments are also attributed to differences in concentration, which might affect species distribution in each study.

Titration of peptide **2** (25 μM) with $Pb(NO_3)_2$ (0–125 μM) yielded a broad LMCT band centered at 320 nm, while peptide **4** displayed a defined LMCT band at 310 nm (Fig. 2B). In contrast, peptide **3** exhibited a weaker LMCT response, with a primary band at 330 nm and a shoulder at 280 nm. Furthermore, the saturation ratio indicates the formation of an equimolar complex (Fig. 2B). These results suggest that in peptides **2** and **4**, all carboxylates and thiols participate in coordination, forming two distinct Pb(II)-binding sites, each likely comprising a thiol–carboxylate pair, as indicated by the single LMCT signal corresponding to this coordination mode. Due to the opposing

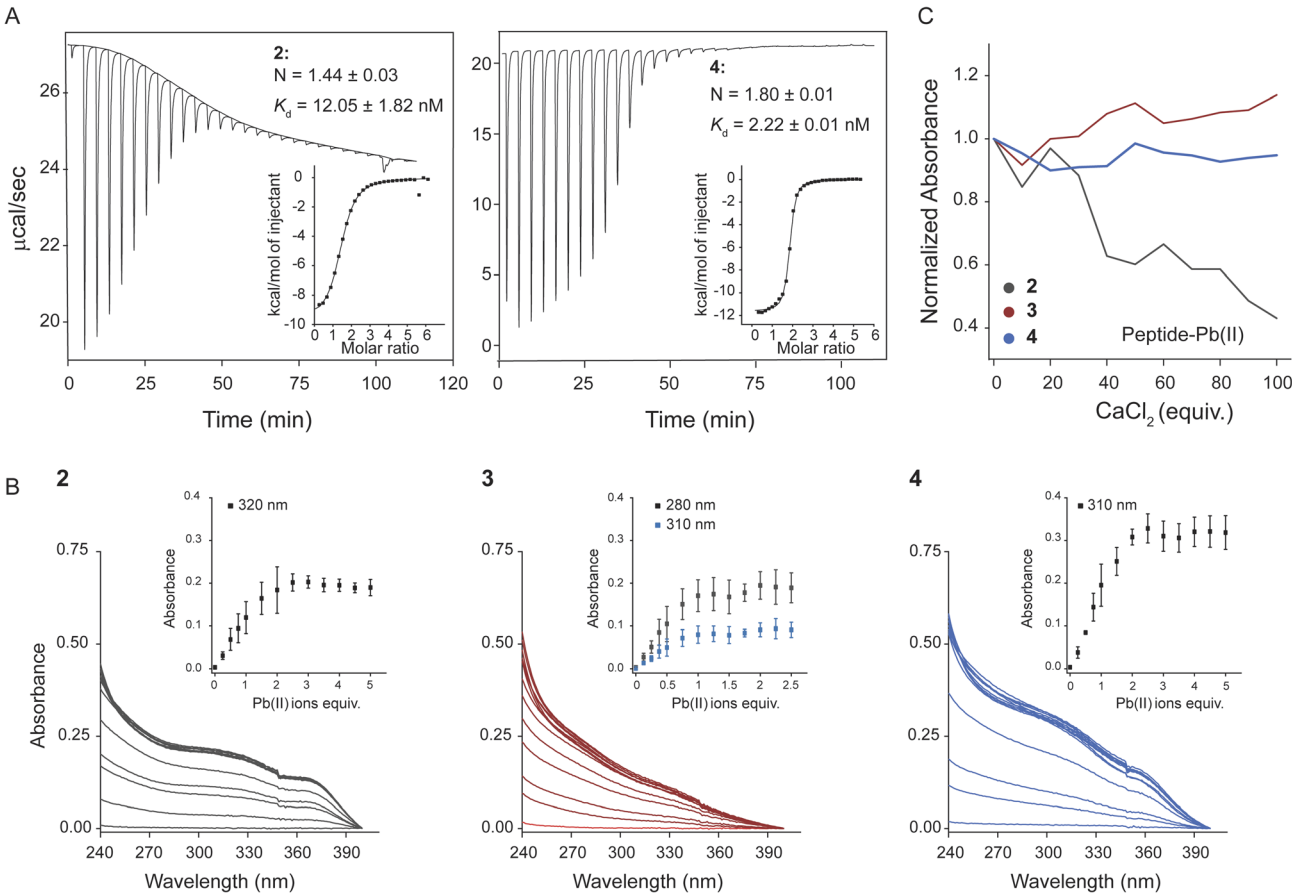

Fig. 2 (A) ITC raw and integrated data for the titration of peptides **2** and **4** with Pb(II) ions. Titrations were performed in 20 mM Tris buffer, pH 6.5, at 25 °C, with $Pb(NO_3)_2$ solution (280 µL; 3.0 mM and 0.6 mM for peptides **2** and **4**, respectively) titrated into the peptide solution (1.8 mL; 100 and 200 µM for peptides **2** and **4**, respectively). (B) UV-titration of peptides **2**–**4** at a concentration of 25 µM with $Pb(NO_3)_2$ in 20 mM Tris buffer at pH 6.5. (C) UV-monitored competitor-titrations of Pb-peptide complexes (25 µM for peptides and 50 µM $Pb(NO_3)_2$) with $CaCl_2$ (0–2.5 mM; 0–100 equiv. to peptide's concentration).

orientation of carboxyl groups in peptide **4**, the two Pb(II) ions are coordinated on separate faces of the peptidic backbone, promoting stable complex formation. Conversely, in peptide **2**, both Pb(II) ions must bind on the same face, likely leading to steric strain and reduced stability. Since complex stability is essential for effective detoxification, this may explain the inability of **2** to rescue Pb-poisoned bacteria and human cells, as has been seen in our *in vitro* evaluations herein.

Selectivity to Pb(II) ions. Although differences in the affinities of peptides **2** and **4** for Pb(II) ions could independently explain their distinct effects on Pb-poisoned cells (Fig. 1D), we further evaluated the selectivity of these peptides toward Pb(II) in the presence of two physiologically relevant metal ions: Zn(II) and Ca(II).[43] These two ions were selected as biologically relevant competitors to Pb(II), each for distinct reasons. Zn(II), although significantly smaller than Pb(II), shares similar coordination preferences, as both ions are classified as borderline Lewis acids that bind to sulfhydryl groups. In contrast, Ca(II) is a hard ion that primarily binds to oxygen-containing ligands and therefore does not expect to bind to Pb-binding molecules (due to significant differences in the hard-soft acid-base theory), but its ionic radius of 112 pm closely resembles that of Pb(II) (119 pm), which can hinder the ability of ligands, including proteins, to effectively distinguish between the two. The latter similarity also results in the accumulation of Pb(II) ions in the brain, leading to neurological impairments.

All three peptides preferentially bound Pb(II) over Zn(II) (Fig. S3–S5).[36] However, only peptides **3** and **4** retained selectivity for Pb(II) in the presence of Ca(II) (Fig. 2C). These findings, which align with our hypothesis of poor metal selectivity for peptide **2**, further support the importance of both metal-ion affinity and selectivity for effective chelation, highlighting the potential of peptide **4** as a candidate chelating agent for Pb poisoning.

As part of the metal selectivity assessment of peptide **4**, we have also determined its affinity to Zn(II) and Ca(II) ions by ITC (Fig. S2).[36] Peptide **4** binds Pb(II) ions 3500 and 5900 times stronger than it binds to Zn(II) and Ca(II) ions, respectively. This is based on the K_d values of 2.22 ± 0.01 nM for Pb(II), 7.8 ± 0.3 µM for Zn(II), and 13.1 ± 1.4 µM for Ca(II) ions (Fig. 2A and S2).[36]

These findings, yet again, indicate the superiority of peptide **4** to tightly and selectively bind Pb(II) ions, thereby inactivating their cellular toxicity *via* complexation.

Computational studies of metal selectivity. To support the experimental observations on metal affinity, selectivity, and hypothesized complexation modes, we performed quantum mechanical DFT-D3//COSMO-RS calculations to gain insights into the interactions of peptides **2**, **3**, and **4** with Pb(II), as well as with two physiologically relevant competing metal ions, Zn(II) and Ca(II).[36,44–47] For each peptide–metal combination, we determined the most stable structures of the hydrated complexes $[M(X)\cdot\{H_2O\}_n]$, where M = Pb(II), Zn(II), or Ca(II), X = peptide **2**, **3**, or **4**, and n = 2–6, depending on the complex. We then calculated the complexation Gibbs free energies ($\Delta G_{complexation}$) of all such complexes. Informed by experimental data, we also investigated binuclear complexes with Pb(II) ions for peptides **2** and **4** (Fig. 3).

The peptides exhibited distinct coordination modes toward Pb(II) ions. Peptide **2** coordinated Pb(II) *via* one thiolate group and two carboxylates, while peptide **3** bound Pb(II) through only the two thiolates. Peptide **4** preferred coordination *via* one of the carboxylate groups of βDAsp and the two thiolate groups. Among these, peptide **4** showed the strongest mononuclear Pb(II) binding, with the lowest $\Delta G_{complexation}$ of −5.5 kcal mol^{-1}. Binuclear complexes of peptides **2** and **4** revealed even higher binding affinities, consistent with ITC and UV-vis experimental data; peptide **4** bound two Pb(II) ions more tightly than its diastereomer, with a total complexation energy of $\Delta G_{complexation}$ of −7.6 kcal mol^{-1}.

These calculations also clarified the metal selectivity observed in the ITC and UV titration experiments. All three peptides exhibited unfavorable (positive) complexation energies for Zn(II), consistent with their low affinity. Peptide **2** exhibited favorable binding to Ca(II) (−2.1 kcal mol^{-1}), in contrast to peptides **3** and **4**, which showed positive complexation energies, indicating weak or no binding.

Overall, the data gathered to this point indicate that high Pb-binding affinity, coupled with metal selectivity, enables the deactivation of toxic Pb(II) ions through complexation, where peptide **4** has been found to suppress its other investigated analogs. We have therefore decided to test its efficacy and safety *in vivo*.

***In vivo* efficacy and safety studies.** Based on the promising complexation data, we evaluated the efficacy of peptide **4** in

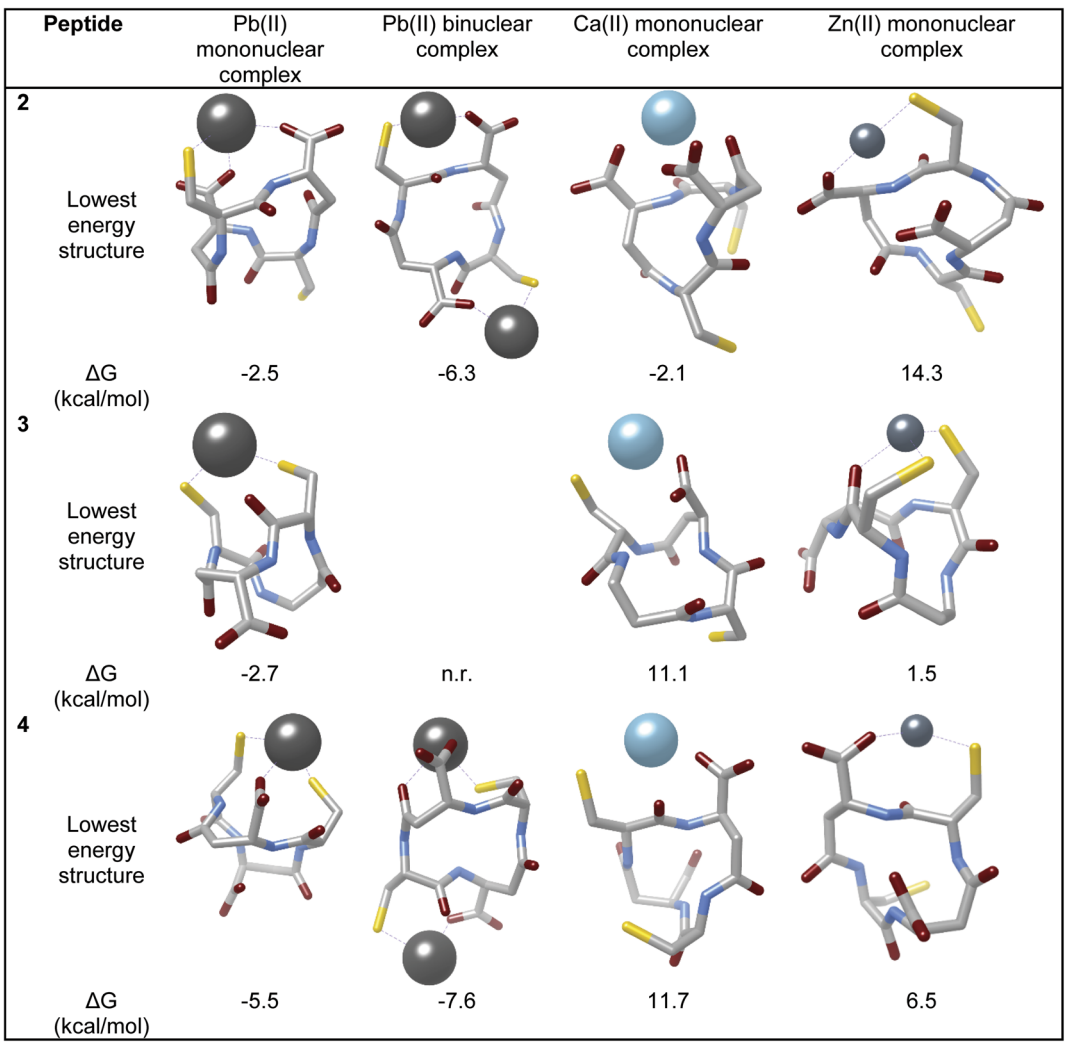

Fig. 3 Computed lowest-energy structures and their energies of **2**–**4** with the Pb(II), Ca(II), and Zn(II) ions (hydrogen atoms and water molecules were omitted for clarity).

promoting Pb(II) chelation and excretion in a murine model of Pb exposure. A total of 45 female C57BL/6 mice (6–8 weeks old) were randomly assigned to three exposure groups ($n = 15$ per group) and given 5, 10, or 20 mM $Pb(Ac)_2$ in drinking water for 7 days (days 1–7), representing low, medium, and high exposure levels (Fig. S7).[36] These three exposure concentrations have been selected based on the threshold of 45 μg dL^{-1} BLL, for which treatment with DMSA can be prescribed. Seven days of exposure to 20 mM Pb(II) solution was thus expected to yield BLLs within this range. On the other hand, the lower exposure levels of 10 and 5 mM Pb(II) solutions have been chosen to study the major unmet medical need of BLLs below 45 μg dL^{-1}, which account for the majority of reported poisoning cases but lack therapeutic options. From day 8 onward, the mice received normal water.

Initial samples (blood, urine, and feces) were collected on day 9, two days after exposure. On day 10, each exposure group was randomly divided into three treatment arms ($n = 5$ animals per arm) and treated *via* daily oral gavage for 15 consecutive days (days 10–24) with: (i) PBS (negative control), (ii) DMSA at 160 μmol kg^{-1} per day, or (iii) peptide **4** at 120 μmol kg^{-1} per day.[48]

Urine was collected 24 hours after the final treatment (day 25) and again on day 31, one week post-treatment. On day 31, all mice were sacrificed, and blood and organs were harvested for *ex vivo* analysis.

The BLLs on day 9 (before the treatment started) were comparable within each exposure group. However, after 15 dosages, mice treated with peptide **4** showed a marked reduction in BLLs, with levels decreased by 55–62% ($p < 0.01$)

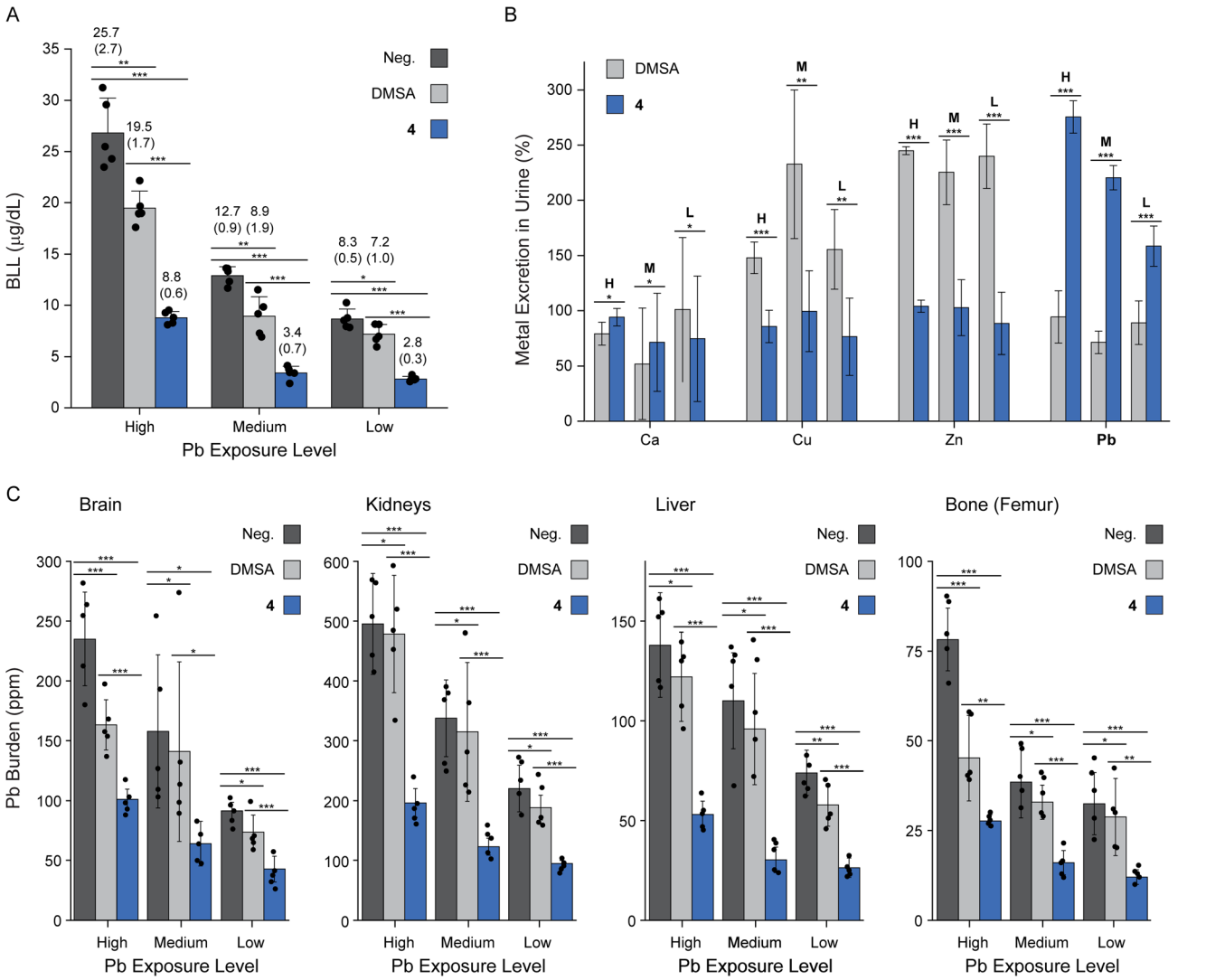

Fig. 4 (A) BLLs of the nine different groups, sub-grouped based on the Pb-exposure levels (high – 20 mM, medium – 10 mM, and low – 5 mM) and the treatment received for 15 consecutive days, one dose daily by oral gavage. Each data point is represented as a black dot. Numbers mark the mean and standard deviation in brackets. (B) Metal ion levels in urine on day 25 (24 hours after the last dose) where four metals were quantified: Ca, Cu, Zn, and Pb. Values are relative to the negative control groups. Pb-exposure levels are marked as H – high, M – medium, and L – low. (C) Pb burden in four key organs: brain, kidneys, liver, and bone (femur) of the nine different groups, sub-grouped based on the Pb-exposure levels on termination day (day 31). *P*-values were calculated based on one-way ANOVA (*$p > 0.05$, **$p < 0.05$, ***$p < 0.01$).

compared to the negative control (Fig. 4A). Notably, peptide **4** also outperformed DMSA in reducing BLLs. This superiority was also evident at lower initial BLLs, where current SOCs are least effective, and the clinical need is greatest.[32,33,49]

We next quantified Pb levels in both urine (Fig. 4B) and feces on day 25 (24 hours after the last dose), alongside three key competing metal ions. While no significant differences were observed in fecal metal content, urinary Pb excretion was significantly increased in mice treated with peptide **4**. To enable direct comparison, urinary metal ion levels were normalized to the corresponding negative control arm for each Pb-exposure group, with values greater than 100% indicating enhanced excretion of the metal ion. Across all exposure levels, peptide **4** induced significantly greater urinary Pb excretion than either PBS (control) or DMSA, reaching up to ~300% in the high-exposure group. In contrast, DMSA was largely ineffective at promoting Pb excretion and instead triggered substantial loss of essential metals, notably Cu and Zn. These results are in line with the reported poor metal selectivity of DMSA.[50] In comparison, peptide **4** preserved physiological levels of these metals, as expected based on the affinity and selectivity examinations conducted on this peptide. Notably, while excretion of essential metals does not necessarily have a negative clinical effect, poor Pb selectivity and competition with high-concentration ions directly reduce the efficacy of Pb removal.

These findings highlight the dual advantages of peptide **4**, which demonstrated both enhanced Pb elimination and high metal-ion selectivity *in vivo*, supporting its potential as a safer and more effective alternative to existing SOC chelation therapies.

Lastly, we quantified Pb levels in key organs affected by Pb exposure, including the brain, kidneys, liver, and femur, with the latter serving as a representative bone compartment due to the known long-term accumulation of Pb in bone tissues[51] (Fig. 4C). Across all exposure levels and organs examined, treatment with peptide **4** resulted in a significant reduction in Pb burden compared to both vehicle controls and DMSA-treated animals. Notably, peptide **4** was also effective in reducing Pb levels in the brain, highlighting its potential to address neurological toxicity, which is a major unmet need in current chelation therapies. Nevertheless, whether peptide **4** crosses the BBB and, if not, what enables it to reduce Pb brain contact, remains elusive.

The *in vivo* efficacy results align with the information gained on peptide **4**, both from the *in vitro* experiments, as well as from the complex's experimental and computational characterizations. All reveal that peptide **4** is designed to stably capture Pb(II) ions, while leaving physiological metal ions intact. Furthermore, peptide **4** enables the active urinary excretion of Pb upon oral administration, outperforming the medication used to treat Pb poisoning.

In addition to metal quantification, all tissue samples also underwent comprehensive macroscopic and histological examination to evaluate potential phenotypic alterations associated with DMSA and peptide **4** treatments. This was conducted on both animals, first those exposed to $Pb(Ac)_2$ and then those receiving a regular water supply. No treatment-related morphological alterations or histopathological changes were observed in any of the experimental groups compared to the controls (Fig. S8 and S9).

Conclusion

This study presents, to our knowledge, the first *in vivo* validated, rationally designed CA exhibiting high selectivity for Pb(II) ions. By fine-tuning a metal-binding peptidic scaffold through systematic structure–activity relationship analyses, we identified peptide **4** as a superior candidate among the tested analogs. Across comprehensive *in vitro* assays, biophysical characterization, selectivity profiling against essential metal ions, and *in silico* modelling, peptide **4** consistently demonstrated exceptional Pb affinity and selectivity, which translated into robust *in vivo* efficacy.

In a short 15 days, once-daily dosing regimen at relatively low doses, peptide **4** outperformed existing treatment options, achieving unprecedented Pb chelation and excretion efficiency. Most notably, peptide **4** significantly reduced Pb levels in the brain, an organ traditionally considered largely inaccessible to chelation therapy due to the BBB.[52] While peptide **4** is not expected to cross the BBB directly due to its high hydrophilicity, these findings suggest that highly efficient systemic Pb clearance can shift metal distribution equilibria sufficiently to promote Pb efflux from the brain. This observation highlights an important and underexplored therapeutic principle: effective detoxification of protected compartments may be achievable without direct chelator penetration, provided that systemic metal binding and elimination are sufficiently strong to drive favorable redistribution.

This concept is particularly significant given the long-standing challenge of treating Pb-associated neurotoxicity, which is often regarded as persistent or irreversible due to Pb sequestration in the CNS. Our results indicate that equilibrium-driven strategies may offer a viable route to indirectly reduce cerebral Pb burden, potentially expanding the scope of chelation therapy beyond conventional assumptions about tissue accessibility.

At the same time, important challenges and open questions remain. The precise mechanisms governing Pb mobilization from the brain, whether through altered plasma-brain gradients, changes in Pb–protein binding, or modulation of transport processes, require further investigation. Long-term efficacy, durability of Pb reduction after treatment cessation, and potential redistribution to other tissues must also be evaluated. Additionally, while peptide **4** demonstrated favorable selectivity against Zn and Ca under the conditions tested, comprehensive chronic safety studies will be essential to assess potential effects on essential metal homeostasis during prolonged administration.

Author contributions

T. A. Mohammed and M. S. Shoshan conceived and designed the experiments and wrote the manuscript; T. A. Mohammed, L. Sauser, E. Pedron, and Y. A. Hodel conducted the experiments; T. Kalvoda and L. Rulíšek performed the computational work; F.

Prisco performed the macroscopic and histopathological examination of the mouse samples; J. P. Holland supervised the animal studies; all authors edited and reviewed the manuscript.

Conflicts of interest

T. A. M. and M. S. S. are the inventors of a patent application owned by the University of Zurich on the work reported in this manuscript. L. S. and M. S. S. are employees of metaLead Therapeutics AG. The other authors declare no conflicts of interest.

Data availability

The data supporting this article are included in the supplementary information (SI). Supplementary information is available. See DOI: https://doi.org/10.1039/d5sc09201a.

Acknowledgements

We thank Prof. Dr Roland K. O. Sigel for generously hosting our team at the University of Zurich and for his invaluable support of our research. The Swiss National Science Foundation (SNF, MSS/PZ00P2_179818), the Innosuisse (Project 104.451 IP-LS), and the University of Zurich (UZH Entrepreneurship Fellowship MSS/BIOEF22-030) are gratefully acknowledged for their financial support. We thank Hana Bušková for her assistance with the calculations of aqueous ions used in this work, and the Histology Laboratory Unit, Institute for Veterinary Pathology, Vetsuisse Faculty, University of Zurich, for excellent technical support. We thank Dr Michaela Thallmair-Honold (animal welfare officer at UZH) for assistance with experimental design. JPH thanks the University of Zurich for financial support. Lastly, we thank the UZH Laboratory Animal Services Center (LASC) and the Department of Chemistry MS Facility for their support.

Notes and references

1 World Health Organization, Data from "Chemicals of major public health concerns.", https://www.who.int/teams/environment-climate-change-and-health/chemical-safety-and-health/health-impacts/chemicals, accessed 3 September 2025.
2 World Health Organization, Data from "Exposure to lead: A major public health concern.", https://iris.who.int/bitstream/handle/10665/372293/9789240078130-eng.pdf?sequence=1, accessed 3 September 2025.
3 N. Rees and R. Fuller, *The toxic truth: Children's exposure to lead pollution undermines a generation of future potential*. UNICEF, 2020, 1–90.
4 H. Needleman, *Annu. Rev. Med.*, 2004, **55**, 209–222.
5 Centers for Disease Control and Prevention, Data from "Updates blood lead reference value for children.", https://www.cdc.gov/lead-prevention/php/news-features/updates-blood-lead-reference-value.html#:~:text=TheBLRVisbasedon,childrento3.5CEBCg2FdL, accessed 3 September 2025.
6 B. P. Lanphear, *et al.*, *Pediatrics*, 2016, 138.
7 M. J. McFarland, M. E. Hauer and A. Reuben, *Proc. Natl. Acad. Sci. U. S. A*, 2021, **11**, 119.
8 A. L. Wani, A. Ara and J. A. Usmani, *Interdiscip. Toxicol.*, 2015, **8**, 55–64.
9 N. C. Papanikolaou, E. G. Hatzidaki, S. Belivanis, G. N. Tzanakakis and A. M. Tsatsakis, *Med. Sci. Monit.*, 2005, **11**(10), RA329–RA336.
10 L. H. Mason, J. P. Harp and D. Y. Han, *BioMed Res. Int.*, 2014, 840547.
11 S. V. Verstraeten, L. Aimo and P. I. Oteiza, *Arch. Toxicol.*, 2008, **82**(11), 789–802.
12 G. Flora, D. Gupta and A. Tiwari, *Interdiscip. Toxicol.*, 2012, **2**, 47–58.
13 M. S. Shoshan, *Chimia*, 2022, **76**, 744–747.
14 J. Aaseth, M. A. Skaug, Y. Cao and O. Andersen, *J. Trace Elem. Med. Biol.*, 2015, **31**, 260–266.
15 J. J. Kim, Y. S. Kim and V. Kumar, *J. Trace Elem. Med. Biol.*, 2019, **54**, 226–231.
16 S. J. S. Flora and V. Pachauri, *Int. Res. J. Publ. Environ. Health*, 2010, **7**, 2745–2788.
17 M. R. Ellis and K. Y. Kane, *Am. Fam. Physician*, 2000, **62**, 545–554.
18 L. Patrick, *Lead Toxicity, A Review of the Literature. Part I: Exposure, Evaluation, and Treatment*, 2006, vol. 11.
19 M. E. Sears, *Sci. World J.*, 2013, 219840.
20 G. A. Bassan and S. Marchesan, *Int. J. Mol. Sci.*, 2023, **24**, 456.
21 Y. Luo, *et al.*, *Int. J. Mol. Sci.*, 2024, **25**, 6717.
22 T. T. L. Nguyen, H. R. Lee, S. H. Hong, J. R. Jang, W. S. Choe and I. K. Yoo, *Appl. Biochem. Biotechnol.*, 2013, **169**, 1188–1196.
23 P. J. Knerr, M. C. Branco, R. Nagarkar, D. J. Pochan and J. P. Schneider, *J. Mater. Chem.*, 2012, **22**, 1352–1357.
24 R. Biondo, F. A. Da Silva, E. J. Vicente, J. E. Souza Sarkis and A. C. G. Schenberg, *Environ. Sci. Technol.*, 2012, **46**, 8325–8332.
25 L. Sauser and M. S. Shoshan, *J. Inorg. Biochem.*, 2020, 111251.
26 W. Su, M. S. Cho, J. Do Nam, W. S. Choe and Y. Lee, *Biosens. Bioelectron.*, 2013, **48**, 263–269.
27 M. Lin, M. Cho, W. S. Choe and Y. Lee, *Electroanalysis*, 2016, **28**, 998–1002.
28 H. R. Lotfi Zadeh Zhad and R. Y. Lai, *Anal. Chem.*, 2018, **90**, 6519–6525.
29 M. Ngu-Schwemlein, W. Gilbert, K. Askew and S. Schwemlein, *Bioorg. Med. Chem.*, 2008, **16**, 5778–5787.
30 S. Gui, Y. Huang, Y. Zhu, Y. Jin and R. Zhao, *ACS Appl. Mater. Interfaces*, 2019, **11**, 5804–5811.
31 T. A. Mohammed, *et al.*, *Angew. Chem., Int. Ed.*, 2021, **60**, 12381–12385.
32 L. Sauser, *et al.*, *Inorg. Chem.*, 2021, **60**, 18620–18624.
33 L. Sauser, T. Kalvoda, A. Kavas, L. Rulíšek and M. S. Shoshan, *ChemMedChem*, 2022, 17.
34 Due to the poor solubility of peptide **1**, which is required for potent chelation therapy, it was not examined on human cells.

35 Peptides **3** and **4** are highly soluble and were therefore tested directly in human cells (Fig. 1C and D), skipping bacterial recovery testing (Fig. 1B).
36 See the SI for further details.
37 N. Percie du Sert, *et al.*, *PLoS Biol.*, 2020, **18**(7), e3000410.
38 The two additional sequences, where (1) R = R' = (R)-COOH and (2) R = (R)-COOH, R' = H, were excluded from this study to minimize complexity and production costs and to remain, as much as possible, within the pool of canonical amino acids.
39 The affinity of peptide **3** was not determined by ITC, as it was inferior in all examined parameters to peptide **4**. Peptide **2**, which was also inferior to peptide 4, was tested for its Pb affinity by ITC to better understand the structure–activity correlation.
40 J. S. Magyar, *et al.*, *J. Am. Chem. Soc.*, 2005, **127**, 9495–9505.
41 G. Zampella, K. P. Neupane, L. De Gioia and V. L. Pecoraro, *Chem.–Eur. J.*, 2012, **18**, 2040–2050.
42 A. Jacquart, R. Brayner, J. M. El Hage Chahine and N. T. Ha-Duong, *Chem. Biol. Interact.*, 2017, **267**, 2–10.
43 Cu(I/II) ions were not examined in the selectivity assessments since (1) such ions are not reported to be replaced or interact with Pb(II) ions; (2) Cu does not appear freely in the bloodstream or cellular environments, but is bound to endogenous proteins and its free concentration is within the aM-fM range; and (3) Cu intracellular concentration is 10–30 times lower than that of Zn. Selectivity against Mg(II) ions was excluded, as this ion, which is significantly smaller than Pb(II), does not share any coordination properties with it. As a result, no known interaction between these two ions or any of Pb's chelating agents is reported.
44 A. D. Becke, *Phys. Rev. A*, 1988, **38**, 3098.
45 J. P. Perdew, *Phys. Rev. B: Condens. Matter Mater. Phys.*, 1986, **33**, 8822(R).
46 S. Grimme, *Chem.–Eur. J.*, 2012, **18**, 9955–9964.
47 A. Klamt, *J. Phys. Chem.*, 1995, **99**, 2224–2235.
48 DMSA daily dose was determined based on the clinical dose and the one administered previously to mice. The daily dose of peptide 4 was determined based on a dose-response preliminary efficacy study by which no significant differences have been observed between the effects of 120 and 160 μmol kg^{-1} per day.
49 O. Gutten and L. Rulíšek, *Inorg. Chem.*, 2013, **52**, 10347–10355.
50 G. Bjørklund, *et al.*, *Molecules*, 2019, **24**, 3247.
51 N. Zoeger, *et al.*, *Osteoarthr. Cartil.*, 2006, **14**, 906–913.
52 M. M. Jones, *et al.*, *Toxicology*, 1994, **89**(2), 91–100.